Invest New Drugs (2011) 29:285–299
DOI 10.1007/s10637-009-9360-3

PRECLINICAL STUDIES

Dibutyltin(IV) complexes containing arylazobenzoate ligands: chemistry, in vitro cytotoxic effects on human tumor cell lines and mode of interaction with some enzymes

Tushar S. Basu Baul · Anup Paul · Lorenzo Pellerito · Michelangelo Scopelliti · Palwinder Singh · Pooja Verma · Andrew Duthie · Dick de Vos · Edward R. T. Tiekink

Received: 5 November 2009 / Accepted: 20 November 2009 / Published online: 11 December 2009
© Springer Science+Business Media, LLC 2009

Summary Dibutyltin(IV) complexes of composition $Bu_2Sn(LH)_2$, where LH is a carboxylate residue derived from 2-[(*E*)-(5-tert-butyl-2-hydroxyphenyl)diazenyl]benzoate (L^1H) with water molecule (**1**), 4-[(*E*)-(5-tert-butyl-2-hydroxyphenyl) diazenyl]benzoate (L^2H) (**2**) and 4-[(*E*)-(4-hydroxy-5-methylphenyl)diazenyl]benzoate (L^3H) (**3**), were synthesized and characterized by spectroscopic (^1H, ^{13}C and ^{119}Sn NMR, IR, ^{119}Sn Mössbauer) techniques. A full characterization was accomplished from the crystal structure of complex **1**. The molecular structures and geometries of the complexes (**1a** i.e. **1** without water molecule and **3**) were fully optimized using the quantum mechanical method (PM6). Complexes **1** and **3** were found to exhibit stronger cytotoxic activity in vitro across a panel of human tumor cell lines viz., A498, EVSA-T, H226, IGROV, M19 MEL, MCF-7 and WIDR. Compound **3** is found to be four times superior for the A498, EVSA-T and MCF-7 cell lines than CCDP (cisplatin), and four, eight and sixteen times superior for the A498, H226 and MCF-7 cell lines, respectively, compared to ETO (etoposide). The mechanistic role of cytotoxic activity of test compounds is discussed in relation to the theoretical results of docking studies with some key enzymes such as ribonucleotide reductase, thymidylate synthase, thymidylate phosphorylase and topoisomerase II associated with the propagation of cancer.

Keywords Anti-cancer drugs · Dibutyltin(IV) compounds · Arylazobenzoate · Spectroscopy · Cell lines · Docking studies

Electronic supplementary material The online version of this article (doi:10.1007/s10637-009-9360-3) contains supplementary material, which is available to authorized users.

T. S. Basu Baul (✉) · A. Paul
Department of Chemistry, North-Eastern Hill University,
NEHU Permanent Campus, Umshing,
Shillong 793 022, India
e-mail: basubaul@nehu.ac.in
e-mail: basubaul@hotmail.com

L. Pellerito · M. Scopelliti
Dipartimento di Chimica Inorganica e Analitica"Stanislao Cannizzaro", Università degli Studi di Palermo,
Viale delle Scienze, Parco D'Orleans II, Edificio 17,
90128 Palermo, Italy

P. Singh · P. Verma
Department of Chemistry, Guru Nanak Dev University,
Amritsar 143005, India

A. Duthie
School of Life & Environmental Science, Deakin University,
Geelong, Victoria 3217, Australia

D. de Vos
Pharmachemie BV,
PO Box 552, 2003 RN, Haarlem, The Netherlands

E. R. T. Tiekink
Department of Chemistry, University of Malaya,
50603 Kuala Lumpur, Malaysia

Introduction

Cisplatin [1–4] was the first inorganic cancer chemotherapeutic agent, and remains a front-line treatment for testicular, ovarian and other cancers. Despite heavy side effects and drug resistance of tumor cells, cisplatin is among the most widely used anti-cancer drugs, and other platinum (II) complexes, such as carboplatin, oxaliplatin and nedoplatin, with improved activity and/or reduced toxicity, are being introduced in therapy. As a result, platinum drugs are playing a major role within established medical treatments of cancers [2, 5, 6]. The wide clinical success of platinum(II) compounds has prompted a great

deal of interest in other platinum and non-platinum metallodrugs (e.g., Sn, Ti, Au, Cu, Ru, Pd) that might exhibit comparable cytotoxic properties accompanied by a different pattern of antitumor specificities and by a more favorable pharmacological and toxicological profile. The current investigative efforts and the state-of-the-art in the field of anticancer metal complexes have been documented in the literature [7–15].

Structural diversity of the organotin(IV) carboxylates is well recognized and a variety of coordination geometries leading to monomeric-, dimeric-, trimeric-, tetrameric-, oligomeric- and polymeric structures have been reported [16–18]. It is generally believed that such structures arise because of combination of steric and electronic factors [19–22]. Furthermore, it has been reported that the size of the carboxylic acids used and stoichiometry of the reactant also play important role in the formation of solid state frameworks. Among the various types of organotin(IV) carboxylates, generally triorganotin(IV) (R_3SnL) and diorganotin(IV) (R_2SnL_2 and $\{[R_2Sn(L)]_2O\}_2$) carboxylates have been investigated in greater extent for their cytotoxic potential [23]. So far, triphenyltin(IV) carboxylates of formulation Ph_3SnL, where L=carboxylate residue, viz., -terebate, -steroidcarboxylate, -benzocrowncarboxylate [23] and those derived from Schiff bases containing amino acetates, e.g., 2-{[(2*Z*)-(3-hydroxy-1-methyl-2-butenylidene)] amino}-4-methyl-pentanoate; 2-{[(*E*)-1-(2-hydroxyphenyl) methylidene]amino}-4-methyl-pentanoate; 2-{[(*E*)-1-(2-hydroxyphenyl)ethylidene]amino}-4-methyl-pentanoate [24], 2-{[(2*Z*)-(3-hydroxy-1-methyl-2-butenylidene)]amino} phenylpropionate; 2-{[(*E*)-1-(2-hydroxyphenyl)methylidene]-amino}phenylpropionate; 2-{[(*E*)-1-(2-hydroxyphenyl)ethylidene]amino}phenylpropionate [25] and arylazobenzoates, e.g., 2-[(*E*)-2-(3-formyl-4-hydroxyphenyl)-1-diazenyl]benzoate; 2-[(*E*)-2-(4-hydroxy-5-methylphenyl)-1-diazenyl]benzoate [26], found to be very active when tested in vitro against human tumor cell lines. In general, the ID_{50} values for the triphenyltin(IV) arylazobenzoates [26] were found to be similar to that of the triphenyltin(IV) complexes of Schiff bases derived from amino acids (e.g., *l*-leucine and phenylalanine) [24, 25] but their advantage lies in prolonged stability in both the solution- and solid-state. Further, the docking studies of triphenyltin(IV) 2-[(*E*)-2-(aryl)-1-diazenyl]benzoates indicated that the azo group nitrogen atoms and formyl, carbonyl and ester oxygen atoms in the ligand moiety also play an important role. They exhibit hydrogen bonding interactions with the active site of amino acids of various enzymes such as ribonucleotide reductase, thymidylate synthase and thymidylate phosphorylase. The higher activity was attributed to the presence of the azo group in the molecules of triphenyltin(IV) complexes [26]. Similar observations were also noted recently for the ruthenium complexes containing azo-ligands which have shown higher activity in comparison to the complexes with non-azo ligands [27]. On the other hand, examples of diorganotin(IV) arylazobenzoates of formulations $R_2Sn(L)_2$ and $\{[R_2Sn(L)]_2O\}_2$ are scanty except for the recent ones where L=5-[(*E*)-2-(aryl)-1-diazenyl]-2-hydroxybenzoate, for which in vitro cytotoxic results were found to be quite promising at least with respect to some of the standard drugs [28, 29].

This investigation focuses on the synthesis and spectroscopic characterization of three new dibutyltin(IV) complexes of compositions, viz., $Bu_2Sn(L^1H)_2.H_2O$ (**1**), $Bu_2Sn(L^2H)_2$ (**2**) and $Bu_2Sn(L^3H)_2$ (**3**), in an attempt to see whether this is a significant variable for docking with various enzymes and to obtain better cytotoxic performances. The ligands used herein show selected variations in the structures, for example, the positions of the caboxylate group (ortho- and para-) in **1** and **2** in which other substituents are held constant, while in **3** nuclear substituent modification of the coupling moiety would hopefully allow some useful conclusions to be made. The molecular structures and geometries of the dibutyltin(IV) compounds (**1a** and **3**) were fully optimized using the semiempirical quantum chemistry method. The molecular docking of **1a** and **3** have been investigated with some selected enzymes and preliminary in vitro cytotoxicity data of complexes (**1–3**) are reported across a panel of human tumor cell lines viz., A498 (renal cancer), EVSA-T (mammary cancer), H226 (non-small-cell lung cancer), IGROV (ovarian cancer), M19 MEL (melanoma), MCF-7 (mammary cancer) and WIDR (colon cancer).

Experimental

Materials and methods

Dibutyltin oxide (Fluka) was used as received. The solvents used in the reactions were of AR grade and dried using standard literature procedures. Benzene was distilled from sodium benzophenone ketyl.

Synthesis and characterization of ligands

Synthesis of 2-[(E)-(5-tert-butyl-2-hydroxyphenyl)diazenyl] benzoic acid (L^1HH')

Ligand L^1HH' was prepared by reacting *o*-carboxybenzenediazonium chloride with 4-*tert*-butyl-phenol in alkaline solution under cold conditions (0–5°C) by the method described in our earlier report [30]. Several crystallizations from methanol yielded red plates of L^1HH'. M.p.: 180–182°C. Anal. calc. for $C_{17}H_{18}N_2O_3$: C, 68.44; H, 6.08; N, 9.39 %. Found C 68.30; H, 6.28; N, 9.59 %. IR absorption (cm^{-1}): 1699 $\nu(OCO)_{asym}$. ^1H and ^{13}C NMR (in $CDCl_3$) gave satisfactory results [30].

The other ligands, viz., L^2HH' and L^3HH' were prepared analogously by reacting *p*-carboxybenzenediazonium chloride with 4-*tert*-butyl-phenol and 2-methylphenol, respectively, in alkaline solution under cold conditions. The characterization and spectroscopic data are presented below.

Synthesis of 4-[(E)-(5-tert-butyl-2-hydroxyphenyl)diazenyl] benzoic acid (L^2HH')

Recrystallized from methanol to give orange crystalline material in 42 % yield. M.p.: 258–260°C. Anal. calc. for $C_{17}H_{18}N_2O_3$: C, 68.44; H, 6.08; N, 9.39 %. Found C 68.18; H, 6.18; N, 9.50 %. IR (cm^{-1}): 1686 $\nu(OCO)_{asym}$. ^{1}H-NMR (DMSO-d_6): δ H: 12.1 [brs, 1H, CO_2H], 8.16 [dd, 2.5 Hz, 8.0 Hz, 2H, H2/6], 7.97 [dd, 2.5 Hz, 8.0 Hz, 2H, H3/5], 7.90 [d, 2.5 Hz, 1H, H6'], 7.45 [dd, 2.5, 8 Hz, 1H, H4'], 6.97 [d, 8 Hz, 1H, H3'], 1.19 [s, 9H, CH_3] ppm. Signal for phenol was exchanged due to presence of water in the solvent. ^{13}C-NMR (DMSO-d_6); δ C: 166.8 [CO_2], 33.6 [C-7'], 30.8 [CH_3], other carbons: 152.8, 150.4, 142.4, 136.7, 132.3, 131.4, 130.4, 126.9, 121.6, 125.9, 117.4 ppm.

Synthesis of 4-[(E)-(4-hydroxy-5-methylphenyl)diazenyl] benzoic acid (L^3HH')

Recrystallized from methanol to give red-orange crystalline material in 60 % yield. M.p.: 234–236°C. Anal. calc. for $C_{14}H_{12}N_2O_3$: C, 65.62; H, 4.72; N, 10.93 %. Found. C, 65.70; H, 4.58; N, 10.88 %. IR (cm^{-1}): 1684 $\nu(OCO)_{asym}$. ^{1}H-NMR (DMSO-d_6): δ H: 13.3 [brs, 1H, CO_2H], 10.4 [brs, 1H, OH], 8.08 [dd, 2.5 Hz, 8.0 Hz, 2H, H2/6], 7.83 [dd, 2.5 Hz, 8.0 Hz, 2H, H3/5], 7.70 [d, 2.5 Hz, 1H, H6'], 7.66 [dd, 2.5, 8 Hz, 1H, H2'], 6.96 [d, 8 Hz, 1H, H5'], 2.48 [s, 3H, CH_3] ppm. ^{13}C-NMR (DMSO-d_6); δ C: 167.7 [CO_2], 16.8 [CH_3], other carbons: 160.7, 155.5, 146.0, 132.6, 131.4, 126.1, 125.8, 124.7, 122.8, 115.8 ppm.

Synthesis and characterization of dibutyltin(IV) complexes

*Synthesis of $Bu_2Sn(L^1H)_2.H_2O$ (**1**)*

A suspension of Bu_2SnO (0.21 g, 0.84 mmol) and L^1HH' (0.50 g, 1.67 mmol) in 50 ml anhydrous benzene was refluxed for 6 h in a flask equipped with a Dean-Stark water separator and a water cooled condenser. After the reaction, a wine-red colored solution was obtained and filtered while hot. The solvent was concentrated on a hot plate and precipitated with petroleum ether. The red colored precipitate was filtered and washed thoroughly with petroleum ether (60–80°C) and dried *in vacuo*. The dried product was dissolved in anhydrous benzene-hexane (v/v 2:1), filtered off to remove any undissolved particles and the filtrate left to crystallize at room temperature. The red–brown crystals were isolated from the mother liquor and dried *in vacuo*. Yield: 46 %. M.p.: 128–130°C. Anal. Found: C, 60.90; H, 6.13; N, 6.90 %. Calc. for $C_{42}H_{54}N_4O_7Sn$: C, 60.66; H, 6.44; N, 6.63 %. IR (cm^{-1}): 1595 $\nu(OCO)_{asym}$. ^{1}H-NMR ($CDCl_3$): δH: Ligand skeleton: 12.5 [brs, 2H, OH], 8.24 [d, 8 Hz, 2H, H3], 7.91 [d, 8 Hz, 2H, H6], 7.84 [d, 2.5 Hz, 2H, H6'], 7.58 [t, 8 Hz, 2H, H5], 7.46 [t, 8 Hz, 2H, H4], 7.31 [dd, 2.5, 8 Hz, 2H, H4'], 6.88 [d, 8 Hz, 1H, H3'], 1.30 [s, 18H, CH_3]; Sn-Bu skeleton: 0.79 [t, 6H, H-4*], 1.35 [m, 4H, H-3*], 1.70 [m, 4H, H-2*], 1.83 [t, 4H, H-1*], ppm. ^{13}C-NMR ($CDCl_3$); δ C: 175.3 [CO_2], 150.8 [C2'], 149.9 [C1], 142.2 [C1'], 137.8 [C4'], 133.1 [C6'], 132.7 [C5], 131.4 [C3], 130.0 [C4], 129.9 [C5'], 127.2 [C2], 118.4 [C3'], 115.8 [C6], 34.1 [C-7'], 31.4 [CH_3]; Sn-Bu skeleton: 13.6 [C-4*], 25.9 [C-3*], 26.3 [C-2*], 26.7 [C-1*] ppm. ^{119}Sn-NMR ($CDCl_3$): −139.5 ppm. ^{119}Sn Mössbauer, mm s^{-1}: δ=1.54, Δ=4.39, Γ_{av}=0.83, ρ =2.85.

*Synthesis of $Bu_2Sn(L^2H)_2$ (**2**)*

Compound **2** was prepared analogously by following the method and conditions described for **1** and using L^2HH' and Bu_2SnO. The orange product was recrystallized from benzene-hexane mixture. Yield: 33%. M.p.: 194–196°C. Anal. Found: C, 61.16; H, 6.45; N, 6.85 %. Calc. for $C_{42}H_{52}N_4O_6Sn$: C, 60.96; H, 6.33; N, 6.77 %. IR (cm^{-1}): 1606 $\nu(OCO)_{asym}$. ^{1}H-NMR ($CDCl_3$); δH: Ligand skeleton: 12.6 [brs, 2H, OH], 8.30 [dd, 2.5 Hz, 8.0 Hz, 4H, H2/6], 7.95 [m, 6H, H3/5 and H6'], 7.43 [dd, 2.5, 8 Hz, 2H, H4'], 6.98 [d, 8 Hz, 2H, H3'], 1.39 [s, 9H, CH_3]; Sn-Bu skeleton: 0.92 [t, 6H, H-4*], 1.46 [m, 4H, H-3*], 1.79 [m, 4H, H-2*], 1.86 [t, 4H, H-1*] ppm. ^{13}C-NMR ($CDCl_3$); δ C: Ligand skeleton: 175.1 [CO_2], 34.1 [C-7'], 31.3 [CH_3], other carbons: 153.5, 150.7, 142.9, 137.1, 131.8, 131.7, 130.1, 128.9, 121.9, 117.8; Sn-Bu skeleton: 13.5 [C-4*], 25.7 [C-3*], 26.5 [C-2*], 26.7 [C-1*] ppm. ^{119}Sn-NMR ($CDCl_3$): –146.3 ppm. ^{119}Sn Mössbauer, mm s^{-1}: δ=1.44, Δ=3.64, Γ_{av}=0.99, ρ =2.53, C-Sn-C=147°.

*Synthesis of $Bu_2Sn(L^3H)_2$ (**3**)*

Compound **3** was prepared analogously by following the method and conditions described for **1** and using L^3HH' and Bu_2SnO. The orange colored product was recrystallized from ethanol. Yield: 53%. M.p.: 132–134°C. Anal. Found: C, 58.28; H, 5.23; N, 7.50 %. Calc. for $C_{36}H_{40}N_4O_6Sn$: C, 58.16; H, 5.42; N, 7.54%. IR (cm^{-1}): 1596 $\nu(OCO)_{asym.}$ ^{1}H-NMR ($CDCl_3$); δ H: Ligand skeleton: not detected [OH], 8.27 [dd, 2.5 Hz, 8.0 Hz, 4H, H2/6], 7.91 [dd, 2.5 Hz, 8.0 Hz, 4H, H3/5], 7.81 [d, 2.5 Hz, 2H, H6'], 7.74 [dd, 2.5, 8 Hz, 1H, H2'], 6.89 [d, 8 Hz, 2H, H5'], 2.34 [s, 6H, CH_3]; Sn-Bu skeleton: 0.89 [t, 6H, H-4*], 1.46 [m, 4H, H-3*], 1.79 [m, 4H, H-2*], 1.87 [t, 4H, H-1*],

ppm. ^{13}C-NMR ($CDCl_3$); δ C: Ligand skeleton: 176.1 [CO_2], 16.3 [CH_3], other carbons: 158.2, 156.1, 147.4, 132.0, 131.2, 126.1, 125.5, 124.2, 122.8, 115.7; Sn-Bu skeleton: 13.9 [C-4*], 26.1 [C-3*], 26.8 [C-2*], 27.1 [C-1*] ppm. ^{119}Sn-NMR ($CDCl_3$): −142.8 ppm. ^{119}Sn Mössbauer, mm s^{-1}: δ=1.41, Δ=3.34, Γ_{av}=0.82, ρ =2.37, C-Sn-C=138°.

Physical measurements

Carbon, hydrogen and nitrogen analyses were performed with a Perkin Elmer 2400 series II instrument. IR spectra in the range 4,000–400 cm^{-1} were obtained on a Perkin Elmer Spectrum BX series FT-IR spectrophotometer with samples investigated as KBr discs. The ^{1}H and ^{13}C spectra were recorded on a Bruker AMX 400 spectrometer and measured at 400.13 and 100.62 MHz, respectively, while ^{119}Sn NMR spectra were recorded either on a Bruker AMX 400 or a Jeol GX 270 spectrometer and measured at 149.18 and 100.75 MHz, respectively. The ^{1}H, ^{13}C and ^{119}Sn chemical shifts were referenced to Me_4Si set at 0.00 ppm, $CDCl_3$ set at 77.0 ppm and Me_4Sn set at 0.00 ppm respectively. The Mössbauer spectra were recorded with a conventional spectrometer operating in the transmission mode. The source was $Ca^{119}SnO_3$ (Ritverc GmbH, St. Petersburg, Russia; 10 mCi), moving at room temperature with constant acceleration in a triangular waveform. The driving system, multi-channel analyser, proportional counter gas detector and the related electronics were purchased from Takes (Ponteranica, Bergamo, Italy). The solid absorber samples, containing *ca.* 0.5 mg cm^{-2} of ^{119}Sn, were held between aluminum foil windows at 77.3 K in a NRD-1258-DMB liquid-nitrogen cryostat (Cryo Industries, USA). The velocity was calibrated using a 10 mCi ^{57}Co Mössbauer source and an α^{57}Fe foil, 4 μm thick, as absorber (both Ritverc GmbH, St. Petersburg, Russia). The isomer shifts are relative to room temperature $Ca^{119}SnO_3$.

Experimental protocol and cytotoxicity tests

The in vitro cytotoxicity test of dibutyltin(IV) compounds **1**–**3** was performed using the SRB test for the estimation of cell viability. The human cancer cell lines examined in the present study were WIDR (colon cancer), M19 MEL (melanoma), A498 (renal cancer), IGROV (ovarian cancer) and H226 (non-small cell lung cancer) belong to the currently used anticancer screening panel of the NCI, USA [31]. The MCF7 cell line is estrogen receptor (ER)+/ progesterone receptor (PgR)+(breast cancer) and the cell line EVSA-T is (ER)-/(Pgr)- (breast cancer). Prior to the experiments, a mycoplasma test was carried out on all cell lines and found to be negative. All cell lines were maintained in a continuous logarithmic culture in RPMI 1640 medium with Hepes and phenol red. The medium was supplemented with 10% FCS, penicillin 100 μg/ml and streptomycin 100 μg/ml. The cells were mildly trypsinized for passage and for use in the experiments. RPMI and FCS were obtained from Gibco (Invitrogen, Paisley, Scotland). SRB, DMSO, Penicillin and streptomycin were obtained from Sigma (St. Louis MO, USA), TCA and acetic acid from Baker BV (Deventer, NL) and PBS from NPBI BV (Emmer-Compascuum, NL).

The test compounds **1**–**3** and reference compounds were dissolved in a concentration of 5 mg/ml in DMSO. Compound **1** did not dissolve immediately in DMSO but it required long vortexing. Compound **2** also had dissolution problem in DMSO. It was first stirred at 37°C and then at 50°C but the compound did not dissolve completely, so the suspension of **2** in DMSO was used to make the dilutions in medium. On the other hand, compound **3** was freely soluble in DMSO. The compounds were subsequently diluted to a final concentration of 250,000 ng/ml in full medium. Cytotoxicity was estimated by the microculture sulforhodamine B (SRB) test [32].

The experiment was started on day 0. On day 0, 150 μl of trypsinized tumor cells (1,500–2,000 cells/well) were plated in 96-wells flat-bottomed micro-titer plates (Cellstar, Greiner Bio-one). The plates were pre-incubated for 48 h at 37°C, 5 % CO_2 to allow the cells to adhere to the bottom. On day 2, a three-fold dilution sequence of ten steps was made in full medium, starting with the 250,000 ng/ml stock solution. Every dilution was used in quadruplicate by adding 50 μl to a column of four wells. This procedure results in the highest concentration of 625,000 ng/ml being present in column 12. Column 2 was used for the blank. To column 1, medium was added to diminish interfering evaporation.

On day 7, the incubation was terminated. Subsequently, the cells were fixed with 10% trichloroacetic acid in PBS and placed at 4°C for an hour. After three washings with tap water, the cells were stained for at least 15 min with 0.4% SRB dissolved in 1% acetic acid. After staining, the cells were washed with 1% acetic acid to remove the unbound stain. The plates were air-dried and the bound stain was dissolved in 150 μl 10 mM tris-base. The absorbance was measured at 540 nm using an automated microplate reader (Labsystems Multiskan MS). The data were used for construction of concentration-response curves and determination of the ID_{50} values by use of Deltasoft 3 software.

The variability of the in vitro cytotoxicity test depends on the cell lines used and the serum applied. With the same batch of cell lines and the same batch of serum the inter-experimental CV (coefficient of variation) is 1–11% depending on the cell line and the intra-experimental CV is 2–4%. These values may be higher with other batches of cell lines and/or serum.

X-ray crystallography

Single crystals suitable for an X-ray crystal-structure determination were obtained from dichloromethane/n-heptane (v/v 1:1) by slow evaporation of the solution of the compound $Bu_2Sn(L^1H)_2.H_2O$ (**1**). Crystal data for **1** i.e. $C_{42}H_{54}N_4O_7Sn$: M=845.58, orthorhombic, $P2_12_12$, a=14.6214(7), b=22.6226(10), c=6.0367(3) Å, V=1996.78 (16) Å^3, Z=2, D_x=1.406, $F(000)$=880, μ=0.694 mm^{-1}. Intensity data were collected at 98(1) K for a red-brown prism (0.08×0.10×0.40 mm) on a Rigaku AFC12κ/SATURN724 CCD using Mo Kα radiation so that θ_{max}=27.5°. There were 4379 unique absorption corrected [33] data (R_{int}=0.023) and 4338 data with $I \geq 2\sigma(I)$. The structure was solved by heavy-atom methods (PATTY in DIRDIF92 [34]) and refined (anisotropic displacement parameters, carbon-bound H atoms in the riding model approximation, and a weighting scheme $w=1/[\sigma^2(F_o^2)+(0.019P)^2+1.861P]$ where $P=(F_o^2+2F_c^2)/3$) with SHELXL-97 on F^2 [35]. The hydroxyl-H atom was located in a difference Fourier map but included in an idealised position. The final R was 0.023 (obs. data) and the wR (all data) was 0.056. The absolute structure was determined on the basis of difference in Friedel pairs included in the data set. The view of the molecule of **1** and supramolecular aggregation are shown in Figs. 1 and 2, which were drawn with 50% probability ellipsoids [36] and DIAMOND [37], respectively.

Crystallographic data (without structure factors) for the structure(s) reported in this paper have been deposited with the Cambridge Crystallographic Data Centre (CCDC) as supplementary publication no. CCDC-744049. Copies of the data can be obtained free of charge from the CCDC (12 Union Road, Cambridge CB2 1EZ, UK; Tel.: +44-1223-336408; Fax: +44-1223-336003; e-mail: deposit@ccdc.cam.ac.uk; Web site: http://www.ccdc.cam.ac.uk).

Computational methods

The molecular structures and geometries of the dibutyltin (IV) compounds (**1a** i.e. **1** without water molecule and **3**) were fully optimized using the semiempirical quantum chemistry method (PM6) [38–42] using the Program CP2K 2.1.7 (Development Version) working with quickstep method [43]. Dockings of compounds **1a** and **3** in the active sites of various enzymes are performed using ArgusLab 4.0.1. [38, 44–46]. This program was also applied for visualization and molecular modeling of the compounds. The three dimensional coordinates of the key enzymes such as ribonucleotide reductase (pdb ID: 4R1R), thymidylate synthase (pdb ID: 2G8D), thymidylate phosphorylase (pdb ID: 1BRW) and topoisomerase II (pdb ID: 1QZR) were obtained from the Internet at the Research Collaboratory for Structural Bioinformatics (RCSB) Protein Data Bank. The docking program implements an efficient grid-based docking algorithm, which approximates an exhaustive search within the free volume of the binding site cavity. The conformational space was explored by the geometry optimization of the flexible ligand (rings are treated as rigid) in combination with the incremental construction of the ligand torsions. Thus, docking occurs between the flexible ligand part of the compounds and enzymes. The ligand orientation is determined by a shape scoring function based on Ascore and the final positions are ranked by lowest interaction energy values. Prior to docking, the ground state was optimized using the PM6QM implemented in the geometry optimization module of pro-

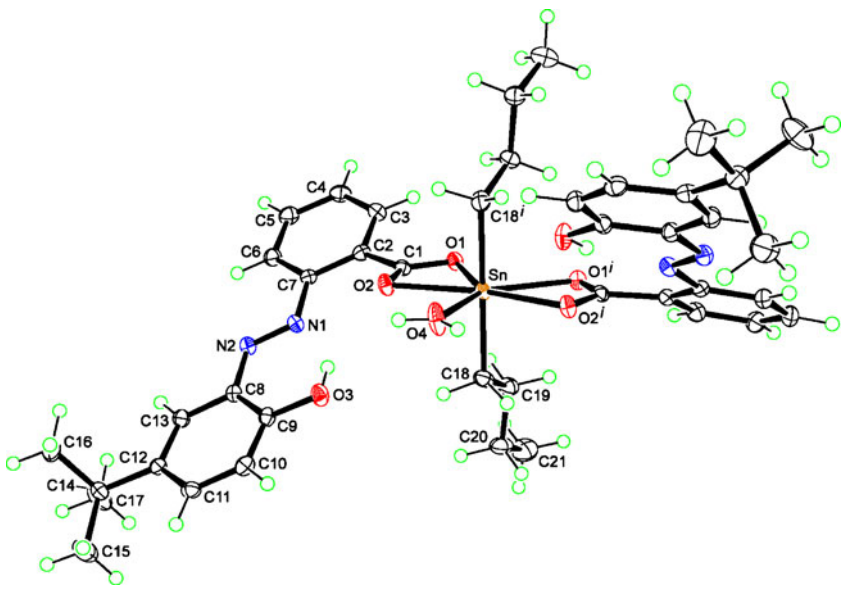

Fig. 1 Molecular structure and crystallographic numbering scheme for **1**. The diagram was drawn with 50% displacement ellipsoids and the atoms indicated with a superscripted *i* are related by the symmetry operation: 1-*x*, 1-*y*, *z*. Selected geometric parameters: Sn–O1 2.3280(16), Sn–O2 2.3334(15), Sn–O4 2.2096(19), N1–N2 1.263(3) Å; O1–Sn–O2 55.85 (5), O1–Sn–O4 136.88(4), O2–Sn–O4 81.07(4), O1–Sn–O1^i 86.23(8), O2–Sn–O2^i 162.14(8), C18–Sn–C18^i 179.53(14)°

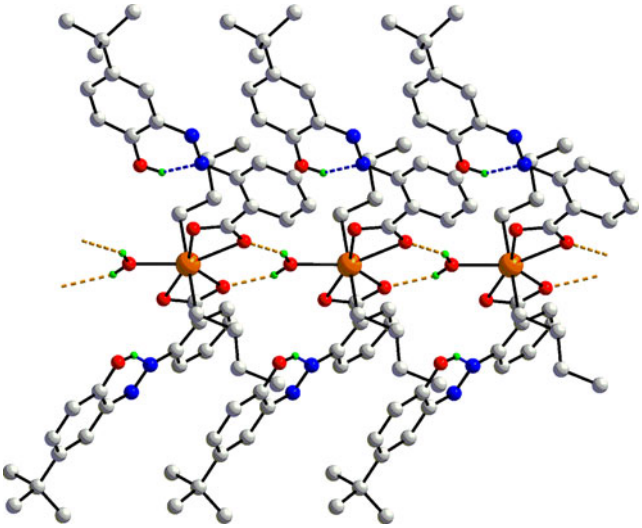

Fig. 2 Supramolecular aggregation leading to a one-dimensional chain in the crystal structure of **1**. Hydrogen bonding is shown as orange (O–H…O) and blue (O–H…N) dashed lines

gram package to confirm that no significant divergence in the conformations of the complexes due to crystal packing effects.

Results and discussion

Synthesis and spectroscopy

Ligands L^1HH'-L^3HH' were prepared using diazo-coupling reactions. L^1HH' was synthesized by reacting *o*-carboxybenzenediazonium chloride with 4-*tert*-butyl-phenol [30] while L^2HH' and L^3HH' were prepared by reacting *p*-carboxybenzenediazonium chloride with 4-*tert*-butyl-phenol and with 2-methylphenol, respectively, in alkaline solution under cold conditions. Recently, one of the ligands, L^1HH' was characterized by NMR and single crystal X-ray diffraction [30]. The reactions between Bu_2SnO and each ligand in a 1:2 ratio, with azeotropic removal of generated water from benzene, produces the new diorganotin(IV) complexes of formulation $Bu_2Sn(LH)_2$ (Complexes **1**–**3**; Scheme 1). The complexes **1**–**3** are colored crystalline solids with well defined melting points, stable in air and soluble in common organic solvents. Analytical purities of the complexes were established by elemental analyses and multinuclear NMR (^1H, ^{13}C and ^{119}Sn) spectroscopic data.

The IR spectra of complexes **1**–**3** displayed a strong sharp band at around 1,600 cm^{-1} which has been assigned to the carboxylate antisymmetric [$\nu_{asym}(OCO)$] stretching vibration, in accord with our earlier reports [47–50]. The assignment of the symmetric [$\nu_{sym}(OCO)$] stretching vibration band could not be made owing to the complex pattern of the spectra. The ^1H and ^{13}C NMR data of the ligands and their complexes **1**–**3** are given in the "Material and Methods" section. The ^1H NMR integration values were completely consistent with the formulation of the products. The ^{13}C NMR spectra of the ligands and complexes **1**–**3** displayed the expected carbon signals. In the ^1H NMR spectra, the signals due to CO_2H of ligands appear in the range 12–13 ppm and were found to be absent in the complexes **1**–**3**, confirming the bonding of the carboxylato group to the Sn atom. The ^{119}Sn NMR spectra of **1**–**3** in $CDCl_3$ solution reveal a sharp signal in the range −140 to −146 ppm, consistent with those reported for other $R_2Sn(O_2CR')_2$ systems [28, 49–53]. The similar range of chemical shifts imply the same coordination arrangement, i. e. a trapezoidal bipyramid, is preserved in all the three complexes. This means that the aqua complex $Bu_2Sn(L^1H)_2.H_2O$ (**1**) dissociates in solution to give $Bu_2Sn(L^1H)_2$ (**1a**), similar to other two complexes $Bu_2Sn(L^2H)_2$ (**2**) and $Bu_2Sn(L^3H)_2$ (**3**).

Scheme 1 Syntheses of dibutyltin(IV) complexes (**1**–**3**) and their structures

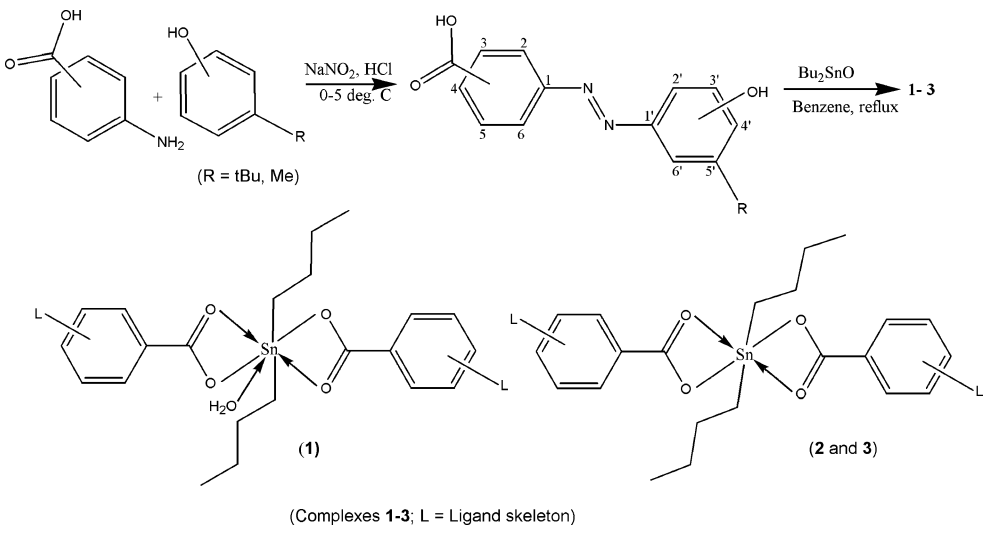

The Mössbauer spectra of the dibutyltin(IV) complexes (**1**–**3**) have been recorded in order to obtain further insight into the structure in the solid state. Typically, one doublet spectra with narrow average full width at half maximum of the resonant peaks (Γ_{av}, 0.82–0.99 mm s^{-1}), characteristic of occurrence of unique tin coordination site, were obtained in all the compounds. From the deconvolution of the obtained spectra, isomer shifts (δ) of 1.54 for **1**, 1.44 for **2**, and 1.41 for **3** mm s^{-1}, typical of organotin(IV) derivatives [54] were extracted. Furthermore, these δ values are higher than the δ of the parent dibutyltin(IV) compound (δ=1.08 mm s^{-1} for Bu_2SnO) [55]. This would suggest that the tin–ligand bond character, in all the complexes, is more covalent than in the parent dibutyltin(IV)oxide [56]. As far as the quadrupole splitting ($|\Delta_{exp}|$) values for the complexes are concerned, the values for **2** (3.64 mm s^{-1}) and **3** (3.34 mm s^{-1}) are indicative of a skew octahedral configuration of the tin atom with *trans*- alkyl groups [54]. The ratio of the quadrupole splitting to isomer shift value ($\rho = |\Delta_{exp}|/\delta$) indicates coordination number greater than four [54].

According to Sham and Brancroft [57], for Sn(IV) complexes containing a R_2Sn(IV) moiety, quadrupole splitting (|Δ|) values depend mainly on highly covalent Sn–C bonds, so that the contributions of the other less covalent bonds can be safely ignored. As a consequence, the relationship between Δ and C–Sn–C bond angles can be expressed according to

$$|\Delta| = -4[R]\left[1 - 3\sin^2\theta\cos^2\theta\right]^{1/2} \quad (1)$$

where [R] is the partial quadrupole splitting value (pqs value) of organic groups bonded to the tin atom, and θ is the C–Sn–C angle. Depending on the coordination number, appropriate [R] values have been successfully used in Eq. 1 to calculate C–Sn–C angles satisfactorily in penta- and hexa-coordinated Sn(IV) compounds [58]. For $Bu_2Sn(L^2H)_2$ (**2**) and $Bu_2Sn(L^3H)_2$ (**3**), C–Sn–C angles have been calculated as 147° and 138°, respectively, (in agreement with the value 129.3° for **3** found by quantum mechanical method (PM6) (Table 1)), clearly indicating distortion from an ideal *trans*-R_2Sn octahedral structure.

Furthermore, the 4.39 mm s^{-1} $|\Delta_{exp}|$ value for the complex $Bu_2Sn(L^1H)_2.H_2O$ (**1**) was found to be higher for a hexa-coordinated organotin(IV) derivative, but is in good agreement with the values found for several previously reported hepta-coordinated organotin(IV) derivatives [59–62], owing to a larger distortion which generally produce greater |Δ | values than hexa- and penta- coordinated ones. Applying Eq. 1 to the experimental |Δ | value and to the crystallographically determined C–Sn–C angle (~180°), it has been possible to measure a partial quadrupole splitting value [R]=−1.10 mm s^{-1} which is in full agreement with previous reports where [R] were found to be −1.08 [60] and −1.09 mm s^{-1} [61].

Crystal structure

The molecular structure of **1** is shown in Fig. 1 and selected geometric parameters are collected in the figure caption. The central tin atom is chelated by two carboxylate anions, a water molecule, and the carbon atoms derived from two butyl groups. The molecule conforms to crystallographic two-fold symmetry with the tin atom and water-oxygen atom lying on the two-fold axis. The carboxylate chelates the tin centre by forming almost equidistant Sn–O bond distances of 2.3280(16) and 2.3334(15) Å; the equivalence of the Sn–O bonds is reflected in the C-O bond distances which are equal within experimental error, *i.e.* 1.268(3) and 1.254(3) Å. The Sn–O bond formed by the water molecule, at 2.2096(19) Å, is slightly shorter than the $Sn–O_{carboxylate}$ bonds. Deprotonation at the carboxylate residue is confirmed by the short N1–N2 bond distance of 1.263(3) Å and the formation of an intramolecular $O_{hydroxyl}–H\ldots N1_{azo}$ hydrogen bond (O3–H3o…N1=1.88 Å, O3…N1=2.597(3) Å with angle subtended at H3o of 142°) along with a weaker $O_{hydroxyl}–H\ldots O2_{carboxylate}$ interaction (O3–H3o…O2=2.33 Å, O3…O2 = 2.974(2) Å, with angle at H3o of 134°). A consequence of these intramolecular hydrogen bonds is the near planarity of the carboxylate ligand as evidenced by the magnitudes of the N1/N2/C8/C9 and C1/C2/C7/N1 torsion angles of 2.6(3) and –8.5(3)°, respectively. The coordination geometry at the tin atom is based on a pentagonal bipyramidal arrangement with the pentagonal plane defined by five oxygen atoms, and with the axial positions occupied by the n-butyl groups; the C–Sn–C axial angle is very nearly linear at 179.53(14)°.

Despite the rather large number of organotin carboxylate structures available in the literature [16], there is only a limited number conforming to the general formula $R_2Sn(O_2CR')_2(OH_2)$ where the carboxylate ligand does not carry functionality capable of forming additional interactions to tin, such as a pyridine-nitrogen atom. There are only four $R_2Sn(O_2CR')_2(OH_2)$ structures and three of these, *i.e.* with *R*=butyl [63, 64] and cyclohexyl [65], having the same structural motif, including the crystallographically imposed two-fold symmetry, as reported herein. The exceptional structure is that of $Me_2Sn(O_2CCF_3)(OH_2)$, *i.e.* featuring the somewhat electron-donating tin-bound methyl groups [66]. Here, the carboxylate ligands form quite asymmetric bonds to tin with two Sn–O bonds, *i.e.* 2.081(3) and 2.205(3) Å, being significantly shorter than the two Sn…O interactions, i.e. 3.146(4) and 2.985(3) Å; the $Sn–O_{water}$ distance is 2.238(3) Å. If the weaker Sn…O interactions are ignored, the coordination geometry is based on a trigonal bipyramidal arrangement with the equatorial positions defined by the

Table 1 Selected bond lengths (Å) and angles (º)[a] for energy minimized structures of the dibutyltin(IV) complexes **1a** and **3**

Bond lengths (Å) and angles (°)	**1a**	**3**	Bond lengths (Å) and angles (°)	1a	3
Sn-O1	2.18	2.16	O2-C1-C2	129.1	126.2
Sn-O2	2.69	2.71	C1-C2-C3	118.1	119.0
Sn-O1^{i}	2.18	2.16	C1-C2-C7	122.9	120.3
Sn-O2^{i}	2.69	2.71	C3- C2-C7	118.9	120.6
O1-C1	1.32	1.32	C2-C7-N1	115.6	–
O2-C1	1.25	1.24	C4-C5-N1	–	125.3
C1-C2	1.48	1.48	C6-C7-N1	124.5	–
C2-C3	1.41	1.40	C6-C5-N1	–	114.0
C3-C4	1.39	1.39	C7-N1-N2	119.5	–
C4-C5	1.40	1.41	C5-N1-N2	–	117.9
C5-C6	1.39	1.41	N1-N2-C8	116.5	117.8
C6-C7	1.41	1.39	N2-C8-C9	127.2	125.0
C7-C2	1.42	1.40	N2-C8-C13	114.3	114.5
C7-N1	1.44	–	C13-C8-C9	118.5	120.4
C5-N1	–	1.45	C8-C9-O3	126.2	–
N1-N2	1.26	1.26	C10-C9-O3	114.2	–
N2-C8	1.42	1.44	C11-C12-C14	122.3	–
C8-C9	1.42	1.41	C13-C12-C14	119.3	–
C9-C10	1.42	1.39	C9-C10-C14	–	120.9
C10-C11	1.38	1.41	C11-C10-C14	–	121.4
C11-C12	1.42	1.41	C10-C11-O3	–	123.3
C12-C13	1.39	1.39	C12-C11-O3	–	114.3
C13-C8	1.42	1.41	O1-Sn-C18	106.4	–
C12-C14	1.53	–	O1-Sn-C15	–	107.4
C10-C14	–	1.49	O2-Sn-C18	86.9	–
C9-O3	1.34	–	O2-Sn-C15	–	87.1
C11-O3	–	2.13	O1-Sn-C18^{i}	106.5	–
Sn-C18	2.13	–	O1-Sn-C15^{i}	–	107.4
Sn-C15	–	2.13	O2-Sn-C18^{i}	86.8	
Sn-C18^{i}	2.13	–	O2-Sn-C15^{i}	–	86.7
Sn-C15^{i}	–	2.13	C18-Sn-C18^{i}	131.9	–
			C15-Sn-C15^{i}	–	129.3
O1-Sn-O2	51.6	51.6	O1^{i} -Sn-C18^{i}	106.5	–
O1^{i}-Sn-O2^{i}	51.6	51.6	O1^{i}-Sn-C15^{i}	–	107.5
Sn-O1-C1	107.9	107.8	O2^{i}-Sn-C18^{i}	87.1	–
Sn-O2-C1	85.6	84.0	O2^{i}-Sn-C15^{i}	–	86.8
O1-C1-C2	116.0	117.3			

[a] Refer to Figs. 3 and 4 for the numbering schemes

methyl groups and an oxygen atom of a carboxylate residue.

The major feature of the note in the crystal packing is the formation of O–H…O hydrogen bonding interactions. As illustrated in Fig. 2, each of the water-bound H4o atoms forms a hydrogen bond with a translationally related carboxylate-O1 atom leading to the formation of supramolecular chains along the *c*-direction, see Fig. S1 (refer to the Supplementary materials) for a packing diagram. The parameters associated with this hydrogen bonding are O4–H4o…O1^{ii}=1.91Å, O4…O1^{ii}=2.657(2) Å, with an angle subtended at H4o of 147° for symmetry operation *ii*: *x*, *y*, 1+*z*.

Quantum chemical calculations

The geometries of the dibutyltin(IV) complexes (**1a** and **3**) were fully optimized using the quantum mechanical method (PM6). Harmonic frequency calculations were performed for all the stationary points to characterize their nature and to ensure that the optimized structures correspond to global minima. The molecular structures of **1a** and **3** were

obtained after full geometry optimization at PM6 levels are shown in Figs. 3 and 4, respectively, while the optimized geometric parameters are collected in Table 1. The experimental geometrical parameters for **1** generally do not match closely with that of calculated values for **1a**, as expected, owing to the different coordination geometry (pentagonal bipyramid) around the tin atom, caused by coordination of the water molecule. Compounds **1a** and **3** have a six-coordinate structure (Figs. 3 and 4). The carboxylate groups on the ligands act as bidentate chelating agents, giving a basal plane around the tin of four asymmetrically coordinated oxygen atoms, whereas the butyl groups are in the axial positions, but pinned back somewhat to produce a skew-trapezoidal bipyramidal structure. Such a configuration is commonly encountered with diorganotin(IV) carboxylates [16]. Diorganotin(IV) compounds of this type exhibiting this structural motif have Sn–O1 values ≤2.2 Å and Sn–O2 values ≥2.5 Å. The corresponding bond lengths observed for **1a** are 2.18 (Sn–O1) and 2.69 (Sn–O2), and for **3** are 2.16 (Sn–O1) and 2.71 (Sn–O2) (Table 1). In addition, **1a** and **3** have the two butyl substituents disposed over the longer Sn–O vectors with C–Sn–C angles of around 130° (**1a**: 131.9° (C18-Sn-C18^{i}) and **3**: 129.3° (C15-Sn-C15^{i})). Since the basic structures and coordination geometry of the dibutyltin(IV) complexes (**1a** and **3**) are similar for the differently substituted ligands, it can be expected that the ligand properties may have direct influences on the stability of the corresponding dibutyltin (IV) complexes, as well as on their cytotoxic activity (see below).

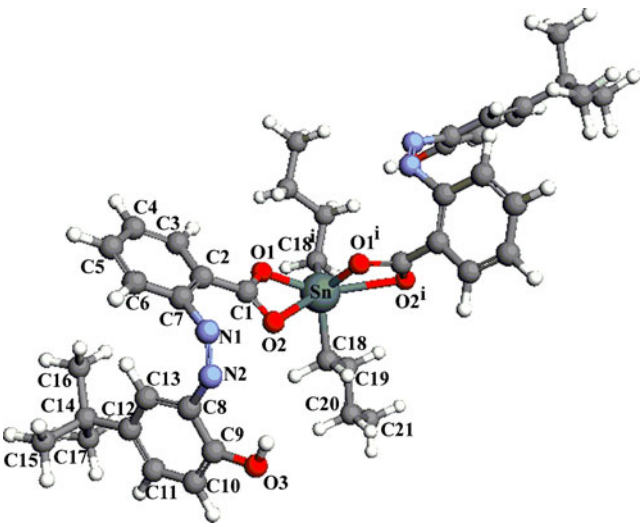

Fig. 3 The structure of $Bu_2Sn(L^1H)_2$ (**1a**) obtained after full geometry optimization

Cytotoxicity studies

The in vitro cytotoxic properties of diorganotin(IV) compounds of formulations such as (a) $Bu_2Sn(L^4H)_2$ (**4**) [28], (b) $\{[Bu_2Sn(L^5H)_2]_2O\}_2$ (**5**) [29], $\{[Bu_2Sn(L^6H)_2]_2O\}_2$ (**6**) [29] and triorganotin(IV) compounds, e.g., (c) $[Ph_3SnL^7H]_n$ (**7**) [26] and $[Ph_3SnL^8H]_n$ (**8**) [26] are reported across a panel of human tumor cell lines viz., A498, EVSA-T, H226, IGROV, M19 MEL, MCF-7 and WIDR as per NCI protocol (Table 2). It should be mentioned herein that the ligand skeleton in all the compounds, i.e. LH is a carboxylate residue where L^4H, 5-[(*E*)-2-(2-methylphenyl)-1-diazenyl]-2-hydroxybenzoate; L^5H, 5-[(*E*)-2-phenyl-1-diazenyl]-2-hydroxybenzoate; L^6H, 5-[(*E*)-2-(4-methylphenyl)-1-diazenyl]-2-hydroxybenzoate, L^7H, 2-[(*E*)-2-(3-formyl-4-hydroxyphenyl)-1-diazenyl]benzoate and L^8H, 2-[(*E*)-2-(4-hydroxy-5-methylphenyl)-1-diazenyl]benzoate all contain an azo group. On the whole, appreciable cytotoxic effects were noted for these set of compounds. However, owing to the limited numbers of compounds studied, it is difficult to define the overall spectrum of the activity of the compounds or their possible selectivity. In the solid state, compounds of formulation (a) have a skew trapezoidal geometry while formulation (b) possesses a centrosymmetric tetranuclear bis(dicarboxylatotetrabutyldistannoxane) frame-work which contain a planar Sn_4O_2 core in which two μ_3-oxo O-atoms connect an Sn_2O_2 ring to two exocyclic Sn-atoms [29] and each tin center has either trigonal bipyramidal or octahedral geometry, depending on the donor atoms. On the other hand, formulation (c) is polymeric, where the Sn atom is trigonal bipyramidal in solid state, but collapses (as revealed from ^{119}Sn NMR spectroscopy) in the solution state to give a monomeric tetrahedral tin species [26].

Among the organotin(IV) compounds of formulations (a–c) described above, the triphenyltin compounds **7** and **8** (formulation (c)) possess highest cytotoxicity and are tetrahedral in solution [26]. It is also reported that the four coordinated tin species have a stronger tendency to increase the coordination numbers by O, S or N donor groups, while five-coordinated species do not undergo further coordination and play no long term role in vivo chemistry of organotin(IV) ester [67–70]. Further, the higher activity of **7** and **8** is attributed to the greater partition coefficient value for triorganotins compared to diorganotins [67, 68]. Recent docking studies indicated that the triphenyltin(IV)-2-[(*E*)-2-(3-formyl-4-hydroxyphenyl)-1-diazenyl]benzoate (**7**) and 2-[(*E*)-2-(4-hydroxy-5-methylphenyl)-1-diazenyl]benzoate (**8**) exhibit hydrogen bonding interactions through azo nitrogen atoms, formyl, carbonyl and ester oxygen atoms of the molecule of triphenyltin compounds with the amino acid residue of the enzymes and thus the presence of an azo functionality in the ligand could be a possible reason for

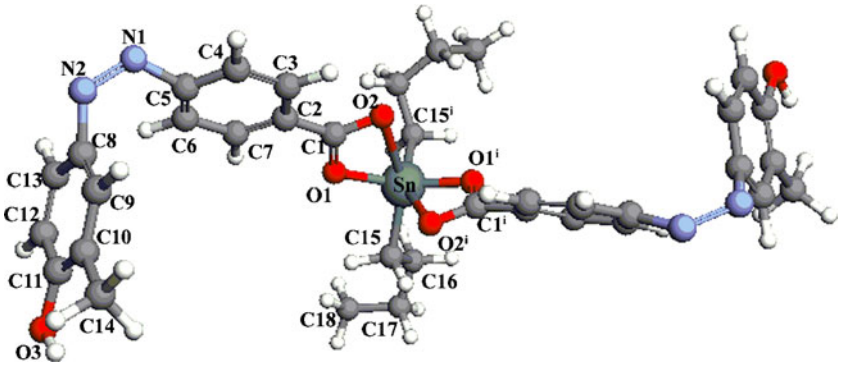

Fig. 4 The structure of $Bu_2Sn(L^3H)_2$ (**3**) obtained after full geometry optimization

enhanced activity [26]. Such observations were also concluded for the ruthenium complexes containing azo-ligands which have shown higher activity in comparison to the complexes with non-azo ligands [26]. Thus, it may be inferred that the activity may depend on the coordination geometry in solution, nature of R groups attached to Sn atom and the skeletal framework of coordinating benzoato ligand.

In view of these information and to rationalize the structure-activity, the three new dibutyltin(IV) complexes **1**–**3** of formulation (a), were investigated for their cytotoxic potential and the results are summarized in Table 2 and the screening results are compared with the results from other organotin(IV) compounds containing arylazobenzoate framework. Under identical conditions, compound **3** displayed better activity than compounds **1** and **2**, across a panel of cell lines. The test compound **3** is found to be far superior to CCDP (cisplatin), and ETO (etoposide), and the activity is four times superior for the A498, EVSA-T and MCF-7 cell lines than CCDP, and four, eight and sixteen times superior for the A498, H226 and MCF-7 cell lines, respectively, compared to ETO. This encouraging cytotoxic

Table 2 In vitro ID_{50} values (ng/ml) of test compounds **1**–**3** along with some reported organotin(IV) azo-compounds against some standard drugs using as cell viability test in seven human tumor cell lines[a]

Test compound[b]	Cell lines						
	A498	EVSA-T	H226	IGROV	M19 MEL	MCF-7	WIDR
$Bu_2Sn(L^1H)_2$ (**1**)	429	134	816	617	374	236	896
$Bu_2Sn(L^2H)_2$ (**2**)	1169	371	1140	1489	901	416	2125
$Bu_2Sn(L^3H)_2$ (**3**)	382	134	497	449	294	162	551
$Bu_2Sn(L^4H)_2$ (**4**) [c] [28]	387	63	337	179	122	124	359
$\{[Bu_2Sn(L^5H)_2]_2O\}_2$ (**5**) [c] [29]	135	14	205	149	52	27	116
$\{[Bu_2Sn(L^6H)_2]_2O\}_2$ (**6**) [c] [29]	140	14	217	155	54	29	115
Ph_3SnL^7H (**7**)[d] [26]	103	49	101	101	104	78	95
Ph_3SnL^8H (**8**)[d] [26]	101	41	104	109	103	92	104
DOX	90	8	199	60	16	10	11
CDDP	2253	422	3269	169	558	699	967
5-FU	143	475	340	297	442	750	225
MTX	37	5	2287	7	23	18	<3.2
ETO	1314	317	3934	580	505	2594	150
TAX	<3.2	<3.2	<3.2	<3.2	<3.2	<3.2	<3.2

[a] *DOX* doxorubicin, *CDDP* cisplatin, *5-FU* 5-fluorouracil, *MTX* methotrexate, *ETO* etoposide and *TAX* paclitaxel

[b] Standard drug reference values are cited immediately after the test compounds under identical conditions. For compounds **1**–**3**, the reference values for CCDP were 1503, 493, 645, 229, 711, 653 and 576 for A498, EVSA-T, H226, IGROV, M19 MEL, MCF-7 and WIDR cell lines, respectively

[c] Reported dibutyltin(IV) compounds (**4**–**6**) have been included for comparison; see refs. 28, 29: LH is a carboxylate residue where L^4H, 5-[(*E*)-2-(2-methylphenyl)-1-diazenyl]-2-hydroxybenzoate; L^5H, 5-[(*E*)-2-phenyl-1-diazenyl]-2-hydroxybenzoate; L^6H, 5-[(*E*)-2-(4-methylphenyl)-1-diazenyl]-2-hydroxybenzoate

[d] Reported triphenyltin(IV) compounds (**7**–**8**) have been included for comparison; see refs. 26: LH is a carboxylate residue where L^7H, 2-[(*E*)-2-(3-formyl-4-hydroxyphenyl)-1-diazenyl]benzoate; L^8H, 2-[(*E*)-2-(4-hydroxy-5-methylphenyl)-1-diazenyl]benzoate

effect may be predictive of in vivo antitumor activity. The lower activities of **1** and **2** compared to **3** may be attributed to the steric crowding of bulky *t*-Bu of the ligand skeleton of **1** and **2** which possibly hinders the binding ability. Further, the cytotoxicity data of **3** is comparable to that reported for compound **4** against A498 cell line**.** However, much better activities were noted for the compounds **5** and **6** with formulation (b) and could be realized due to the presence of two tin centres in the molecule. Notably, the triphenyltin(IV) compounds **7** and **8** with formulation (c) were found to be better performers than compounds of other formulations ((a) and (b)), showing relevant cytotoxic properties against all the cell lines used. However, the variations in in vitro cytotoxicity among various formulations (a–c) across tumor cell lines may also be due to different kinetic and mechanistic behavior. Overall, the results reported strongly support the view that the organotin (IV) compounds are potent cytotoxins and deserve greater attention as potential anticancer agents.

Docking study

The encouraging cytotoxic activity for the test compounds **1**–**3** across a panel of cell lines viz., A498, EVSA-T, H226 IGROV, M19 MEL, MCF-7 and WIDR and current information acquired from the docking studies of compounds **7** and **8** performed with some enzymes [26], prompted us to carry out molecular docking studies of **1a** and **3** (formulation (a)) to understand the complex-protein interactions. The docking studies were performed with some enzymes such as ribonucleotide reductase, thymidylate synthase, thymidylate phosphorylase and topoisomerase II and their interactions with **1a** and **3** are shown in Figs. 5, 6, 7, 8, 9 and 10. The docking programme is validated by docking ADP in the active site of enzyme ribonucleotide reductase and a close overlapping between the docked ligand and the native ligand was observed [26]. The docking studies reveal that dibutyltin(IV) compounds **1a** and **3** interact with enzymes at various sites and their hydrogen bonding interactions are given in Table 3. They show appreciable interactions with ribonucleotide reductase, thymidylate synthase and thymidylate phosphorylase, however, they do not enter the active site of topoisomerase II.

Docking study shows that the compounds **1a** and **3** are masked inside the active site of ribonucleotide reductase (Figs. 5 and 6) and both exhibit hydrogen bonding interactions through azo nitrogen atoms, hydroxyl and carbonyl groups with amino acid residues of the enzyme. The interactions of **1a** with ribonucleotide reductase are better than those exhibited by **3**.

Similarly, compound **1a** when docked in the active site of thymidylate synthase also shows hydrogen bonding interactions with R23, L195 and S219 through carbonyl

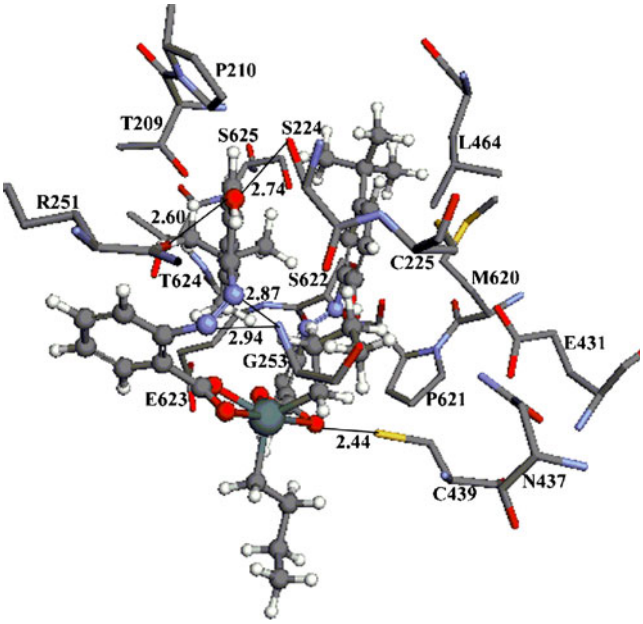

Fig. 5 $Bu_2Sn(L^1H)_2$ (**1a**) docked into the binding site of the enzyme ribonucleotide reductase (4R1R). Hydrogen bonding interactions between the various groups of **1a** and amino acid residues are shown. Hydrogen atoms are omitted for clarity

oxygen atoms while azo nitrogen and hydroxyl oxygen atoms interact with R218 amino acid residues of the enzyme (Fig. 7). On the other hand, compound **3** shows more hydrogen bonding interactions compared to **1a** with active site of thymidylate synthase. Compound **3** exhibits hydrogen bonding interactions through azo nitrogen atoms, OH and carbonyl groups with S219, C198, S219, R23 and W85 amino acid residues of the enzyme (Fig. 8).

Likewise, the dockings of compounds **1a** and **3** in the active sites of thymidylate phosphorylase show the H-bonding interactions between the various groups of this compound and amino acid residues as shown in Figs. 9 and 10. Compound **3** interacts through the nitrogen atoms of the azo groups with the amino acids G1113, R1168 and I1180, and using carbonyl oxygen atoms, it forms hydrogen bonds with the amino acids Y1165 and T1117. The hydroxyl groups form hydrogen bonds with the amino acids G1119 and R1168 and besides this, it also forms hydrogen bonds with D1122 and R1168 which are not visible in the present view of Fig. 10. On the other hand, both the azo group nitrogen atoms as well as two carbonyl oxygen atoms of compound **1a** show hydrogen bond interactions with the amino acid Y1165. Nitrogen atoms of an azo group form hydrogen bonds with L1114 and G1113 while a carbonyl oxygen atom interacts with T1117. Unlike compound **3**, only one hydroxyl oxygen atom is involved in the hydrogen bond formation with the amino acids G1113 and R1112.

Therefore, on the basis of docking studies, it is inferred that the anticancer activities of compounds **1a** and **3** might

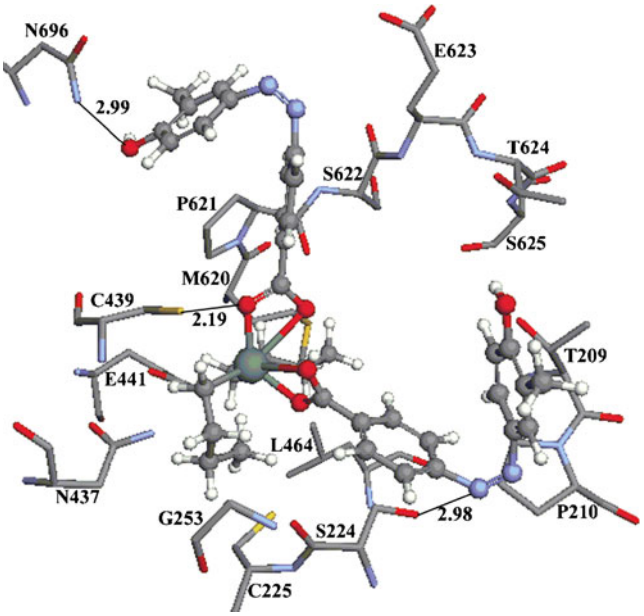

Fig. 6 $Bu_2Sn(L^3H)_2$ (**3**) docked into the binding site of the enzyme ribonucleotide reductase (4R1R). A number of hydrogen bonding interactions between compound **3** and amino acid residues are shown. Hydrogen atoms are omitted for clarity

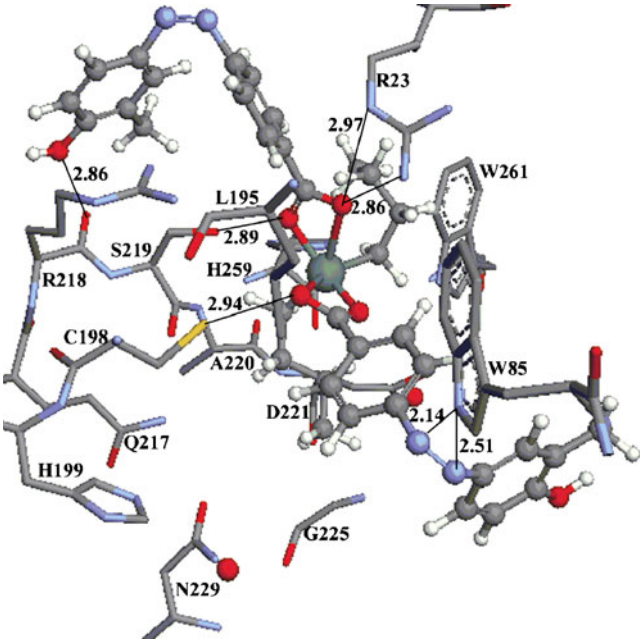

Fig. 8 $Bu_2Sn(L^3H)_2$ (**3**) docked into the binding site of the enzyme thymidylate synthase (2G8D). Hydrogen bonding interactions between the ligand part of the molecule of **3** and amino acid residues are shown. Hydrogen atoms are omitted for clarity

be emanating from their interactions with enzymes ribonucleotide reductase, thymidylate synthase and thymidylate phosphorylase. The docking studies also indicate that the azo group nitrogen atoms and hydroxyl and carbonyl oxygen atoms in the ligand moiety play an important role during the dockings of the dibutyltin(IV) compounds into the active sites of various enzymes as discussed above. Nevertheless, the possibility of coordination through tin beyond the active site of the enzymes cannot be ruled out completely. It is very difficult to envisage the role of such atoms in binding proteins in relation to improved cytotoxic activity. However, the exact reasons for such activity cannot be deduced at this stage from the available data.

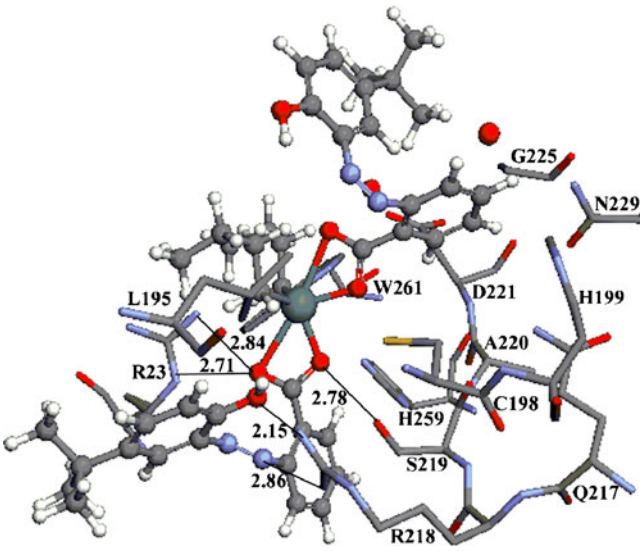

Fig. 7 $Bu_2Sn(L^1H)_2$ (**1a**) docked into the binding site of the enzyme thymidylate synthase (2G8D). Hydrogen bonding interactions between various groups of **1a** and amino acid residues are shown. Hydrogen atoms are omitted for clarity

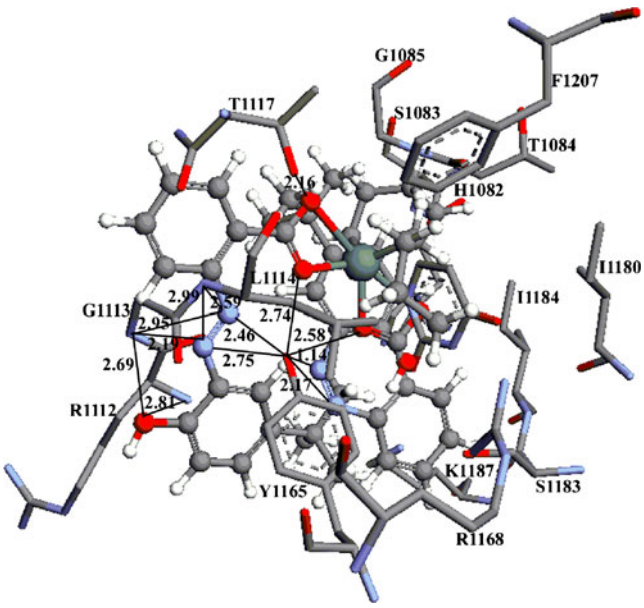

Fig. 9 $Bu_2Sn(L^1H)_2$ (**1a**) docked into the binding site of the enzyme thymidylate phosphorylase (1BRW) showing hydrogen bonding interactions through azo nitrogen, hydroxyl and carbonyl oxygen atoms with various amino acid residues. Hydrogen atoms are omitted for clarity

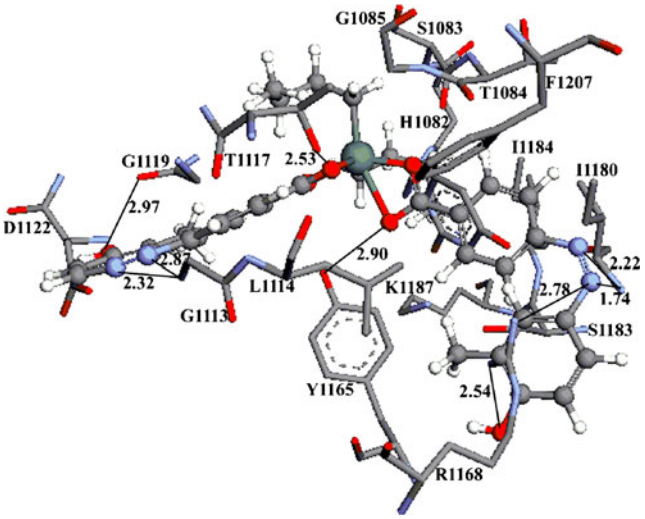

Fig. 10 $Bu_2Sn(L^3H)_2$ (**3**) docked into the binding site of the enzyme thymidylate phosphorylase (1BRW) showing hydrogen bonding interactions through azo nitrogen, hydroxyl and carbonyl oxygen atoms with various amino acid residues. Hydrogen atoms are omitted for clarity

Conclusions and outlook

Three dibutyltin(IV) complexes of formulation $Bu_2Sn(LH)_2$ where LH is arylazobenzoate ligand were synthesized to investigate the role of ligands on the cytotoxic properties of some human tumor cell lines, viz., A498, EVSA-T, H226, IGROV, M19 MEL, MCF-7 and WIDR and to realize the binding capabilities toward some enzymes such as ribonucleotide reductase, thymidylate synthase, thymidylate phosphorylase and topoisomerase II. The molecular structures and geometries of compounds **1a** and **3** were fully optimized using the quantum mechanical method (PM6). Both dibutyltin(IV) compounds **1** and **3** show very high cytotoxicity when tested in vitro across seven human tumor cell lines indicating their high potential as an anti-cancer drug. Under identical conditions, compound **3** displayed better activity than compounds **1** and **2** across a panel of cell lines. The lower activities of **1** and **2** compared to **3** may be attributed to the steric crowding of bulky *t*-Bu of the ligand skeleton of **1** and **2** which possibly hinders the binding ability. Thus, the cytotoxicity of the compounds depends on the nature of ligand constitution and shows different activity. Nevertheless, the presence of the azo group is required for anticancer activity. The docking studies indicated that the azo group nitrogen atoms and hydroxyl and carbonyl oxygen atoms of the dibutyltin(IV) compounds are responsible for interacting with various key enzymes that take part in the synthesis of raw materials for DNA and its replication. The geometrical feature and size of the molecule of organotin(IV) complexes seem to play

Table 3 Hydrogen bonding interactions of dibutyltin(IV) compounds **1a** and **3** with ribonucleotide reductase (4R1R), thymidylate synthase (2G8D) and thymidylate phosphorylase (1BRW)

Compound		Amino acids involved in hydrogen bonding					
Compd. No.	Groups	4R1R		2G8D		1BRW	
		Amino acid residue	Bond distances (Å)	Amino acid residue	Bond distances (Å)	Amino acid residue	Bond distances (Å)
1a	Azo group nitrogen atom(s)	G253	2.74, 2.87	R218	2.86	Y1165	2.46, 2.75
						L1114	1.14, 2.17
						G1113	2.59, 2.99
							2.95, 2.19
	Carbonyl oxygen atom(s)	C439	2.44	S219	2.78	Y1165	2.74, 1.14
				R23	2.71, 2.84	T1117	2.16
	Hydroxyl group oxygen atom(s)	R251	2.60	R218	2.15	G1113	2.69
		C225	2.74			R1112	2.81
3	Azo group nitrogen atom(s)	S224	2.98	W85	2.14, 2.51	G1113	2.32, 2.87
						R1168	2.78
						I1180	2.22, 1.74
	Carbonyl oxygen atom(s)	C439	2.19	C198	2.94	Y1165	2.90
				S219	2.89	T1117	2.53
				R23	2.97, 2.86		
	Hydroxyl group oxygen atom(s)	N696	2.99	R218	2.14, 2.51	G1119	2.97
						R1168	2.54, 1.57
						D1122	0.96, 2.76

an important role in binding with enzymes. The cytotoxic properties of **1** and **3** were compared with triphenyltin(IV) compounds (**7** and **8**) of cognate systems. The cytotoxicity results demonstrated that the structural modification in coordination geometry and Sn-R groups in **1**–**3** did not improve the cytotoxicity toward cell lines compared to **7** and **8**. Data from the present study suggests complex **3** merits further investigation as a new drug and may be suitable candidate for modification in order to improve cytotoxic and dissolution properties. Further work in this area is underway.

Acknowledgements The financial support of the Department of Science & Technology, New Delhi, India (Grant No.SR/S1/IC-03/2005,TSBB and SR/S1/OC-11A/2006, PS), of the Università degli Studi di Palermo, Italy (Grants ORPA079E5M and ORPA0737W2) and the University Grants Commission, New Delhi, India through SAP-DSA, Phase-III, are gratefully acknowledged. The in vitro cytotoxicity experiments were carried out by Ms. P. F. van Cuijk in the Laboratory of Translational Pharmacology, Department of Medical Oncology, Erasmus Medical Center, Rotterdam, The Netherlands, under the supervision of Dr. E. A. C. Wiemer and Prof. Dr. G. Stoter.

References

1. Abu-Surrah AS, Kettunen M (2006) Platinum group antitumor chemistry: design and development of new anticancer drugs complementary to cisplatin. Curr Med Chem 13:1337–1357
2. Barnes KR, Lippard SJ (2004) Metal complexes in tumor diagnosis and as anticancer agents. Met Ions Biol Syst 42:143–177
3. Cepeda V, Fuertes MA, Castilla J, Alonso C, Quevedo C, Perez JM (2007) Biochemical mechanisms of cisplatin cytotoxicity. Anticancer Agents Med Chem 7:3–18
4. Yang P, Guo M (1999) Interactions of organometallic anticancer agents with nucleotides and DNA. Coord Chem Rev 185–186:189–211
5. Reedijk J (2003) New clues for platinum antitumor chemistry: kinetically controlled metal binding to DNA. Proc Natl Acad Sci USA 100:3611–3616
6. Wang D, Lippard SJ (2005) Cellular processing of platinum anticancer. Nat Rev Drug Discov 4:307–320
7. Sigel A, Sigel H (2004) Metal ions in biological systems. Marcel Dekkar, New York
8. Jakupec M, Keppler BK (2004) In: Sigel A, Sigel H (eds) Metal ions in biological systems. Marcel Dekker, New York
9. Alessio E, Mestroni G, Bergamo A, Sava G (2004) Ruthenium antimetastatic agents. Curr Top Med Chem 4:1525–1535
10. Sigel A, Sigel H (2005) Metal ions in biological systems. Wiley, New York
11. Gielen M, Tiekink ERT (eds) (2005) Metallotherapeutic drug and metal-based diagnostic agents. Wiley, Chichester, England
12. Ang WH, Dyson PJ (2006) Classical and non-classical ruthenium-based anticancer drugs: towards targeted chemotherapy (review). Eur J Inorg Chem 4003–4018
13. Bruijnincx PCA, Sadler PJ (2008) New trends for metal complexes with anticancer activity. Curr Opin Chem Biol 12:197–206
14. Tiekink ERT (2008) Anti-cancer potential of gold complexes. Inflammopharmacol 16:138–142
15. Hadjikakou SK, Hadjiliadis N (2009) Antiproliferative and anti-tumor activity of organotin compounds. Coord Chem Rev 253:235–249
16. Tiekink ERT (1994) The rich diversity in tin carboxylate structures. Trends Organomet Chem 1:71–116
17. Tiekink ERT (1991) Structural chemistry of organotin carboxylates: a review of the crystallographic literature. Appl Organomet Chem 5:1–21
18. Chandrasekhar V, Nagendran S, Baskar V (2002) Organotin assemblies containing Sn–-O bonds. Coord Chem Rev 235:1–52
19. Buntine MA, Hall VJ, Kosovel FJ, Tiekink ERT (1998) Influence of crystal packing on molecular geometry: a crystallographic and theoretical investigation of selected diorganotin systems. J Phy Chem A 102:2472–2482
20. Willem R, Verbruggen I, Gielen M, Biesemans M, Mahieu B, Basu Baul TS, Tiekink ERT (1998) Correlating Mossbauer and solution- and solid-state ^{117}Sn NMR data with X-ray diffraction structural data of triorganotin 2-[(*E*)-2-(2-Hydroxy-5-methylphenyl)-1-diazenyl]benzoates. Organometallics 17:5758–5766
21. Dakternieks D, Duthie A, Smyth DR, Stapleton CPD, Tiekink ERT (2003) Steric control over molecular structure and supramolecular association exerted by tin- and ligand-bound groups in diorganotin carboxylates. Organometallics 22:4599–4603
22. Prabusankar G, Murugavel R (2004) Hexameric organotincarboxylates with cyclic and drum structures. Organometallics 23:5644–5647
23. Gielen M, Tiekink ERT (eds) (2005) Metallotherapeutic drug and metal-based diagnostic agents: ^{50}Sn Tin compounds and their therapeutic potential. Wiley, Chichester, pp 421–439 (and references therein)
24. Basu Baul TS, Basu S, de Vos D, Linden A (2009) Amino acetate functionalized Schiff base organotin(IV) complexes as anticancer drugs: synthesis, structural characterization, and in vitro cytotoxicity studies. Invest New Drugs 27:419–431
25. Basu Baul TS, Masharing C, Ruisi G, Jirásko R, Holčapek M, de Vos D, Wolstenholme D, Linden A (2007) Self-assembly of extended Schiff base amino acetate skeletons, 2-{[(2Z)-(3-hydroxy-1-methyl-2-butenylidene)]amino}phenylpropionate and 2-{[(*E*)-1-(2-hydroxyaryl)alkylidene]amino}phenylpropionate skeletons incorporating organotin(IV) moieties: synthesis, spectroscopic characterization, crystal structures, and in vitro cytotoxic activity. J Organomet Chem 692:4849–4862
26. Basu Baul TS, Paul A, Pellerito L, Scopelliti M, Singh P, Verma P, de Vos D (2009) Triphenyltin(IV) 2-[(*E*)-2-(aryl)-1-diazenyl] benzoates as anticancer drugs: synthesis, structural characterization, in vitro cytotoxicity and study of its influence towards the mechanistic role of some key enzymes. Invest New Drugs. doi:10.1007-s10637-009-9293-x
27. Corral E, Hotze ACG, den Dulk H, Leczkowska A, Rodger A, Hannon MJ, Reedijk J (2009) Ruthenium polypyridyl complexes and their modes of interaction with DNA: is there a correlation between these interactions and the antitumor activity of the compounds? J Biol Inorg Chem 14:439–448
28. Basu Baul TS, Rynjah W, Willem R, Biesemans M, Verbruggen I, Holčapek M, de Vos D, Linden A (2004) Dibutyltin(IV) complexes of the 5-[(E)-2-(Aryl)-1-diazenyl]-2-hydroxybenzoic acid ligand: an investigation of structures by X-ray diffraction, solution and solid state tin NMR, electrospray ionisation MS and assessment of in vitro cytotoxicity. J Organomet Chem 689:4691–4701
29. Basu Baul TS, Rynjah W, Rivarola E, Lyčka A, Holčapek M, Jirásko R, de Vos D, Butcher RJ, Linden A (2006) Synthesis and characterization of bis[dicarboxylatotetraorganodistannoxane] units involving 5-[(E)-2-(aryl)-1-diazenyl]-2-hydroxybenzoic acids: an investigation of structures by X-ray diffraction, NMR, electrospray ionization MS and assessment of in vitro cytotoxicity. J Organomet Chem 691:4850–4862
30. Basu Baul TS, Paul A, Arman HD, Tiekink ERT (2008) 2-[(*E*)-(5-tert-Butyl-2-hydroxyphenyl)diazenyl]benzoic acid. Acta Crystallogr Sect. E 64:o2125

31. Boyd MR (1989) Status of the NCI preclinical antitumor drug discovery screen. Principles and practice of oncology, vol 3. Lippincott, Philadelphia, pp 1–12
32. Keepers YP, Pizao PR, Peters GJ, Ark-Otte JV, Winograd B, Pinedo HM (1991) Comparison of the sulforhodamine B protein and tetrazolium (MTT) assays for in vitro chemosensitivity testing. Eur J Cancer 27:897–900
33. Higashi T (1995) ABSCOR. Rigaku Corporation, Tokyo, Japan
34. Beurskens PT, Admiraal G, Beurskens G, Bosman WP, García-Granda S, Smits JMM, Smykalla C (1992) The DIRDIF program system, technical report of the Crystallography Laboratory. University of Nijmegen, The Netherlands
35. Sheldrick GM (2008) A short history of SHELX. Acta Crystallogr A A64:112–122
36. Johnson CK (1976) ORTEP II, Report ORNL-5136. Oak Ridge National Laboratory, Oak Ridge, TN
37. Brandenburg K (2006) DIAMOND. Crystal impact GbR, Bonn, Germany
38. Stewart JJP (1989) Optimization of parameters for semiempirical methods: I. Method. J Comput Chem 10:209–220
39. Stewart JJP (1989) Optimization of parameters for semiempirical methods: II. Applications. J Comput Chem 10:221–264
40. Stewart JJP (1991) Optimization of parameters for semiempirical methods: III. Extension of PM3 to Be, Mg, Zn, Ga, Ge, As, Se, Cd, In, Sn, Sb, Te, Hg, Tl, Pb, and Bi. J Comput Chem 12:320–341
41. Stewart JJP (2004) Optimization of parameters for semiempirical methods IV. Extension of MNDO, AM1, and PM3 to more main group elements. J Mol Model 10:155–164
42. Stewart JJP (2007) Optimization of parameters for semiempirical methods V: Modification of NDDO approximations and application to 70 elements. J Mol Model 13:1173–1213
43. VandeVondele J, Krack M, Mohamed F, Parrinello M, Chassaing T, Hutter J (2005) Quickstep: fast and accurate density functional calculations using a mixed Gaussian and plane waves approach. Comp Phys Comm 167:103–128
44. ArgusLab 4.0.1: Thompson MA, Planaria Software LLC, Seattle, WA, http://www.argusLab.com
45. Protein Data Bank, <http://www.rcsb.org/pdb/>
46. Wang R, Lai L, Wang S (2002) Further development and validation of empirical scoring functions for structure-based binding affinity prediction. J Comput Aided Mol Des 16:11–26
47. Basu Baul TS, Pyke SM, Sarma KK, Tiekink ERT (1996) Crystal and molecular structure of aquatriphenyltin 2-(3-formyl-4-hydroxyphenylazo)benzoate. Main Group met. Chem. 19:807–814
48. Basu Baul TS, Dhar S, Pyke SM, Tiekink ERT, Rivarola E, Butcher R, Smith FE (2001) Synthesis and characterization of triorganotin (IV) complexes of 5-[(*E*)-2-(aryl)-1-diazenyl]-2-hydroxybenzoic acids. Crystal and molecular structures of a series of triphenyltin 5-[(*E*)-2-(aryl)-1-diazenyl]-2-hydroxybenzoates (aryl=phenyl, 2-methylphenyl, 3-methylphenyl and 4-methoxyphenyl). J Organomet Chem 633:7–17
49. Basu Baul TS, Dhar S, Rivarola E, Smith FE, Butcher R, Song X, McCain M, Eng G (2003) Synthesis and characterization of some dibutylbis{5-[(E)-2-(aryl)-1-diazenyl]-2-hydroxybenzoato}tin(IV) compounds. Toxicity studies of di- and tri-organotin complexes on the second instar of Aedes aegypti mosquito larvae. Appl Organomet Chem 17:261–267
50. Basu Baul TS, Rynjah W, Rivarola E, Pettinary C, Linden A (2005) Synthesis and characterization of the first diorganotin(IV) complexes containing mixed arylazobenzoic acids and having skew trapezoidal bipyramidal geometry. J Organomet Chem 690:1413–1421
51. Otera J, Hinoishi T, Kawabe Y, Okawara R (1981) ^{119}Sn, ^{13}C, and ^{1}H NMR studies on six-coordinate dimethyltin bis(chelate) compounds. Chem Lett 10:273–274
52. Lockhart TP, Manders WF (1986) Structure determination by NMR spectroscopy. Dependence of |2 J(119Sn, 1H)| on the Me-Sn-Me angle in methyltin(IV) compounds. Inorg Chem 25:892–895
53. Lockhart TP (1988) Solution and solid-state structures of di-n-butyltin 3-thiopropionate. X-ray crystal structure determination of the cyclic hexamer. Organometallics 7:1438–1443
54. Barbieri R, Huber F, Pellerito L, Ruisi G, Silvestri A (1998) In: Smith PJ (ed) Chemistry of tin: ^{119}Sn Mössbauer studies on tin compounds. Blackie, London, pp 496–540
55. Greenwood NN, Gibb TC (1971) Mössbauer spectroscopy. Chapman & Hill, London
56. Donaldson JD, Grimes SM, Pellerito L, Girasolo MA, Smith PJ, Cambria A, Famà M (1987) Thermal behaviour, ^{119}Sn Mössbauer and IR spectroscopic studies of some diorganotin(IV)carbohydrates. Polyhedron 6:383–386
57. Sham TK, Bancroft GM (1975) Tin-119 Mossbauer quadrupole splittings for distorted dimethyltin(IV) structures. Inorg Chem 14:2281–2283
58. Bancroft GM, Kumar Das VG, Sham TK, Clark MG (1976) Additive model for ^{119}Sn Mössbauer quadrupole splitting in five-co-ordinate organotin(IV) compounds. J Chem Soc, Dalton Trans 643–654
59. Szorcsik A, Nagy L, Sletten J, Szalontai G, Kamu E, Fiore T, Pellerito L, Kalman E (2004) Preparation and structural studies on dibutyltin(IV) complexes with pyridine mono- and dicarboxylic acids. J Organomet Chem 689:1145–1154
60. Szorcsik A, Nagy L, Deak A, Scopelliti M, Fekete ZA, Csaszar A, Pellerito C, Pellerito L (2004) Preparation and structural studies on the $^{t}Bu_2Sn$(IV) complexes with aromatic mono- and dicarboxylic acids containing hetero {N} donor atom. J Organomet Chem 689:2762–2769
61. Pelizzi C, Pelizzi G, Tarasconi P (1983) Synthesis and characterization by IR spectroscopy and x-ray diffraction of a quinazoline-complex of dibutyldichlorotin(IV). Polyhedron 2:145–147
62. Di Nicola C, Galindo A, Hanna JV, Marchetti F, Pettinari C, Pettinari R, Rivarola E, Skelton BW, White AH (2005) Synthesis and spectroscopic and X-ray structural characterization of R_2Sn^{IV}-oxydiacetate and -iminodiacetate complexes. Inorg Chem 44:3094–3102
63. Xueqing S, Zhiqiang Y, Qinglan X, Jinshan L (1998) Synthesis, structures and in vitro antitumor activity of some germanium-substituted di-*n*-butyltin dipropionates. J Organomet Chem 566:103–110
64. Ng SW, Chen W, Zainudin A, Kumar Das VG, Yip W-H, Wang R-J, Mak TCW (1991) Crystal structure of *trans*-C_2SnO_5 pentagonal bipyramidal dibutylbis(phenylacetato)tin(IV) hydrate. J Crystallogr Spectros Res 21:39–43
65. Dakternieks D, Kuan FS, Tiekink ERT (2001) X-ray structure of di(Acetato)-aqua-di(cyclohexyl)tin(IV). Main Group Met Chem 24:291–292
66. Mahon MF, Molloy KC, Stanley JE, Rankin DWH, Robertson HE, Johnson BF (2005) Atmospheric pressure deposition of fluorine-doped SnO_2 thin films from organotin fluorocarboxylate precursors. Appl Organomet Chem 19:658–671
67. Molloy KC (1989) In: Hartley FR (ed) Bioorganotin compounds in the chemistry of metal carbon bond, vol 5. Wiley, New York (Chapter 11)
68. Hook JM, Linahan BM, Taylor RL, Tiekink ERT, Von Gorkom N, Webster LK (1994) Phenyltin diethyldithiocarbamates: solid state and solution structures and in vitro anti-tumour activity. Main Group Met Chem 17:293–311
69. Willem R, Dalil H, Biesemans M, Martins JC, Gielen M (1999) The reaction of di-n-butyltin oxide with hexafluoro-2, 2-bis(4-carboxyphenyl)propane. Appl Organomet Chem 13:605–608
70. Danish M, Alt Helmut G, Badshah A, Ali S, Mazhar M, Nazar-ul-Islam (1995) Organotin esters of 3-(2-furanyl)-2-propenoic acid: their characterization and biological activity. J Organomet Chem 486:51–56